



CHALMERS
UNIVERSITY OF TECHNOLOGY

Syntheses and Crystal Structures of Two Metal-Organic Frameworks Formed from Cd²⁺ Ions Bridged by Long, Flexible

Downloaded from: <https://research.chalmers.se>, 2025-01-19 23:25 UTC

Citation for the original published paper (version of record):

Plater, M., De Silva, B., Foreman, M. et al (2024). Syntheses and Crystal Structures of Two Metal-Organic Frameworks Formed from Cd²⁺ Ions Bridged by Long, Flexible 1,7-*bis*(4-Pyridyl)heptane Ligands with Different Counter-Ions. CRYSTALS, 14(12). <http://dx.doi.org/10.3390/cryst14121105>

N.B. When citing this work, cite the original published paper.

Article

Syntheses and Crystal Structures of Two Metal–Organic Frameworks Formed from Cd²⁺ Ions Bridged by Long, Flexible 1,7-*bis*(4-Pyridyl)heptane Ligands with Different Counter-Ions

M. John Plater *, Ben M. De Silva †, Mark R. St J. Foreman ‡ and William T. A. Harrison 

Department of Chemistry, University of Aberdeen, Aberdeen AB24 3UE, UK; foreman@chalmers.se (M.R.S.J.F.)

* Correspondence: m.j.plater@abdn.ac.uk

† Current address: W. Sam White Building, Peterseat Drive, Altens, Aberdeen AB12 3HT, UK.

‡ Current address: Nuclear Chemistry/Industrial Materials Recycling, Chalmers University of Technology, 412 96 Göteborg, Sweden.

Abstract: The ethanol–water layered syntheses and crystal structures of the coordination polymers [Cd(C₁₇H₂₂N₂)₂(H₂O)₂]·2(ClO₄)·C₁₇H₂₂N₂·C₂H₅OH **2** and [Cd(C₁₇H₂₂N₂)₂(NO₃)₂] **3** are reported, where C₁₇H₂₂N₂ is a flexible spacer, 1,7-*bis*(4-pyridyl)heptane. In compound **2**, *trans*-CdO₂N₄ octahedral nodes are linked by pairs of bridging ligands to result in [001] looped polymeric chains. The chains stack in the [100] direction to form (010) pseudo layers. Sandwiched between them are secondary sheets of free ligands, perchlorate ions and ethanol solvent molecules. Hydrogen bonds between these species help to consolidate the structure. Compound **3** contains *trans*-CdO₂N₄ octahedral nodes as parts of regular 4⁴ nets, which propagate in the (103) plane. Three independent nets are interpenetrated.

Keywords: cadmium(II); MOF; coordination polymer; flexible ligand; interpenetrated network

Citation: Plater, M.J.; De Silva, B.M.; Foreman, M.R.S.J.; Harrison, W.T.A. Syntheses and Crystal Structures of Two Metal–Organic Frameworks Formed from Cd²⁺ Ions Bridged by Long, Flexible 1,7-*bis*(4-Pyridyl)heptane Ligands with Different Counter-Ions. *Crystals* **2024**, *14*, 1105. <https://doi.org/10.3390/cryst14121105>

Academic Editor: Jesús Sanmartín-Matalobos

Received: 11 December 2024

Revised: 18 December 2024

Accepted: 21 December 2024

Published: 23 December 2024



Copyright: © 2024 by the authors. Licensee MDPI, Basel, Switzerland. This article is an open access article distributed under the terms and conditions of the Creative Commons Attribution (CC BY) license (<https://creativecommons.org/licenses/by/4.0/>).

1. Introduction

Dipyridyl ligands, in which a pair of pyridine (py) rings are linked by a flexible alkyl chain [py–(CH₂)_{*n*}–py (*n* ≥ 2)], are effective species for constructing metal–organic frameworks (MOFs) and coordination networks [1–10] but appear to be understudied compared to dicarboxylate linkers. For example, the ligand 1,4-*bis*(4-pyridyl)butane (C₁₄H₁₆N₂) has been crystallised with Cu²⁺ cations and glutarate ions, forming a two-dimensional grid in which the copper ions are held in pairs by four bridging carboxylate groups, and the nitrogen ligands coordinate at the two apical sites of the dimers to form infinite sheets in [Cu₂(C₅H₆O₄)₂(C₁₄H₁₆N₂)]·2(CH₃CN) (Cambridge Structural Database ref. code ECINEM) [1]. The same ligand has been crystallised hydrothermally with Cd²⁺ ions and dicarboxylate anions, forming “helicates” in [Cd(C₁₄H₁₆N₂)(C₁₀H₈O₄)(H₂O)]·H₂O (MUHQAI), in which the metal ions adopt trigonal–bipyramidal coordination geometries [3]. When Zn²⁺ ions and benzotriazole-5-carboxylic acid are combined with 1,4-*bis*(4-pyridyl)butane, an unusual double-layer framework topology arises in [Zn₂(C₇H₃N₃O₂)₂(C₁₄H₁₆N₂)]·2(DMF)·5(H₂O) (DMF = dimethylformamide, C₃H₇NO) (TITBOP), which incorporates tetrahedral ZnN₃O nodes [4].

The next member of this ligand series, 1,5-*bis*(4-pyridyl)pentane (C₁₅H₁₈N₂), can be crystallised with several divalent metal ions, including cobalt, nickel, copper and cadmium. The Co²⁺ (DITYAH), Ni²⁺ (DITYEL) and Cu²⁺ (DITXUA) compounds are isostructural, with the formula [M(C₁₅H₁₈N₂)₂(NO₃)₂] [6], and consist of interpenetrated three-dimensional networks with the charge-balancing nitrate ions bonded to the metal ions, which adopt *trans*-MN₄O₂ coordination geometries. The cobalt and nickel octahedra are almost regular, while the copper octahedra show typical Jahn–Teller elongations of the bonds to the axial

O atoms. Combining cadmium ions with 1,5-*bis*(4-pyridyl)pentane and different counterions lead to strikingly different structures: $[\text{Cd}_2(\text{C}_{15}\text{H}_{18}\text{N}_2)_3(\text{NO}_3)_4] \cdot \text{H}_2\text{O}$ (LOPNUZ) [2] contains distorted CdO_4N_3 pentagonal bipyramids arising from the coordination of three ligands and two chelating nitrate ions: the ligands link the metal ions into infinite sheets. In $[\text{Cd}(\text{C}_{15}\text{H}_{18}\text{N}_2)_2(\text{H}_2\text{O})_2] \cdot 2(\text{ClO}_4) \cdot \text{C}_{17}\text{H}_{22}\text{N}_2 \cdot \text{C}_2\text{H}_5\text{OH}$ (TOKCON), where perchlorate ions provide charge balance, a completely different structure featuring a squashed two-dimensional 4^4 net with linking *trans*- CdN_4O_2 nodes arises, where the O atoms are parts of water molecules. The ClO_4^- ions and “free” (uncoordinated) ligand molecules accept $\text{O}-\text{H} \cdots \text{O}$ and $\text{O}-\text{H} \cdots \text{N}$ hydrogen bonds, respectively, from the water molecules [7].

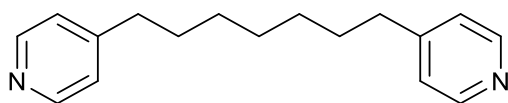
Several structures containing 1,6-*bis*(4-pyridyl)hexane ($\text{C}_{16}\text{H}_{20}\text{N}_2$) as the linking ligand are known. Manganese(II) cations, pairs of *O,O'*-chelating hexafluoro-acetylacetonato anions and bridging $\text{C}_{16}\text{H}_{20}\text{N}_2$ ligands combine together to generate zigzag chains containing *cis*- MnO_4N_2 octahedra in $[\text{Mn}(\text{C}_{16}\text{H}_{20}\text{N}_2)_2(\text{C}_5\text{HO}_2\text{F}_6)_2]$ (WAWDEG) [9], whereas in $[\text{Mn}(\text{C}_{16}\text{H}_{20}\text{N}_2)_2(\text{NCS})_2(\text{C}_2\text{H}_6\text{O})_2]$ (XIBYIQ) [10], the Mn^{2+} ions are coordinated by two *N*-bonded thiocyanate anions, two ethanol solvent molecules and two ligands to generate similar zigzag chains but with *cis*- MnO_2N_4 octahedral nodes. Combining Cu^{2+} with 1,6-*bis*(4-pyridyl)hexane and nitrate counter-ions leads to the very complex structure of $[\text{Cu}(\text{C}_{16}\text{H}_{20}\text{N}_2)_3(\text{NO}_3)_2] \cdot [\text{Cu}(\text{C}_{16}\text{H}_{20}\text{N}_2)_2(\text{H}_2\text{O})(\text{NO}_3)]_2 \cdot 2(\text{NO}_3) \cdot \text{C}_2\text{H}_5\text{OH}$ (ODAHEG) [8], which contains two types of infinite chains in which the Jahn–Teller distorted copper ions are bonded to four ligand N atoms, nitrate O atoms and water molecules. One chain is “looped” (two bridging ligands connect every adjacent pair of metal ions), but the other has one bridging ligand and one “dangling” ligand only bonded to the copper atom from one of its N atoms. The striking structure of $[\text{Cu}_2(\text{C}_{16}\text{H}_{20}\text{N}_2)_4(\text{H}_2\text{O})_2] \cdot 4(\text{NO}_3) \cdot \text{C}_{16}\text{H}_{20}\text{N}_2 \cdot \text{C}_2\text{H}_5\text{OH} \cdot 2\text{H}_2\text{O}$ (ODAHIK) [8] with the same ligand and counter-ion is completely different and consists of CuN_4O square pyramids connected by the bridging ligands into a fourfold interpenetrated three-dimensional network. The difference between ODAHEG and ODAHIK might arise due to the incorporation of uncoordinated water molecules from crystallisation into the latter structure, although this could hardly be predicted from an inspection of the formulae. Finally, in $[\text{Cd}(\text{C}_{16}\text{H}_{20}\text{N}_2)_2(\text{NO}_3)_2]$ (LOPPAH), the combination of cadmium ions, nitrate ions and $\text{C}_{16}\text{H}_{20}\text{N}_2$ ligands leads to a novel structure featuring inclined, interpenetrating 4^4 grids with octahedral CdN_4O_2 nodes [2].

To sum up, an important consequence of using neutral dipyridyl ligands as the metal-ion linkers rather than anions such as dicarboxylates is the requirement for charge-balancing anions, which, as noted above, may exert their own significant influence on the structure and prevent porosity [2,6–8]. Linkers with a longer, flexible spacer unit might give rise to elusive interpenetrated networks because of the greater space associated with the metal-ion coordination sphere in an infinite network [6]. Conversely, the longer alkyl chain might also result in disorder, which can hinder crystallographic studies. Either four pyridine nitrogen atoms might coordinate equatorially to the metal ion (giving a metal-to-ligand ratio of 1:2 as in most of the structures described above), with two counter-ions (most commonly nitrate or perchlorate) or water molecules coordinating apically, or six nitrogen atoms might coordinate octahedrally accompanied by uncoordinated counter-ions as in $[\text{Cd}(\text{C}_{12}\text{H}_{12}\text{N}_2)_3] \cdot 2(\text{ClO}_4)$ (IDAJUS) [$\text{C}_{12}\text{H}_{12}\text{N}_2 = 2$ -*bis*(4-pyridyl)ethane], where the metal-to-ligand ratio is 1:3 and a striking high-symmetry, triply interpenetrated network of infinitely extending cube-like ReO_3 topology building units arises [11]. The literature on *bis*(4-pyridyl)alkanes and M(II) ions was reviewed by us in 2007 [6]. It showed that the most common topologies are one-dimensional ribbons and two-dimensional nets, and two-dimensional or three-dimensional coordination networks are rare from these ligands.

The following novel papers are all relevant to this work because they incorporate pyridyl donors into spacers which bridge between metal ions, rigid or flexible [12–32].

As part of our ongoing studies in this area, we now describe the solvent-layering syntheses and crystal structures of two new coordination polymers prepared from 1,7-*bis*(4-pyridyl)heptane ($\text{C}_{17}\text{H}_{22}\text{N}_2$; *bph*) **1** (Figure 1) and cadmium(II) perchlorate or cadmium(II) nitrate, *viz.*, $[\text{Cd}(\text{C}_{17}\text{H}_{22}\text{N}_2)_2(\text{H}_2\text{O})_2] \cdot 2(\text{ClO}_4) \cdot \text{C}_{17}\text{H}_{22}\text{N}_2 \cdot \text{C}_2\text{H}_5\text{OH}$ **2** and $[\text{Cd}(\text{C}_{17}\text{H}_{22}\text{N}_2)_2(\text{NO}_3)_2]$

3, which shows the dramatic effect of changing the anion in this type of coordination network. The synthesis of the ligand was described in reference [6].



1 1,7-bis(4-pyridyl)heptane

Figure 1. Structure of 1,7-bis(4-pyridyl)heptane.

2. Experimental

2.1. Synthesis and Characterisation

Warning:

[Testimony from Mark R. St J. Foreman]

It is important to use KNH_2 , not NaNH_2 for large scale reactions. The formation of NaNH_2 is much more exothermic than the formation of the KNH_2 . This is thought to be based on lattice energies. I have had some truly scary moments in life making sodium amide but when I summoned up the courage to use potassium amide I found it was far safer to make. I did not have problems with liquid ammonia boiling violently. Also, the initial rate of reaction of solutions of potassium in liquid ammonia with the iron catalyst it much higher, I have never had a problem with unreacted potassium building up in the liquid ammonia but with sodium things can be a bit tricky.

1,7-bis(4-pyridyl)heptane [33]:

A flange flask equipped with a compressed air-driven mechanical stirrer and a cold finger condenser was assembled hot and allowed to cool while being purged with oxygen-free nitrogen gas. After cooling to room temperature, a mixture of solid carbon dioxide and acetone was added to the cold finger condenser. Into this flask, we decanted liquid ammonia (2 L). Potassium metal (23.4 g) was cut up and slowly added to liquid ammonia, which was gently refluxing in a flange flask. After the addition of the first sliver of potassium, a small amount of iron(III) chloride was added to form the catalyst for the reaction of ammonia with the solvated electron to form the potassium amide (KNH_2). After all the potassium had been reacted, the slurry of potassium amide was cooled to $-78\text{ }^\circ\text{C}$ using a cold bath made of solid carbon dioxide and acetone. After allowing the slurry to be stirred for one hour, the dropwise addition of a solution of 4-methylpyridine (60 mL) in diethyl ether (50 mL) was made. After allowing the mixture to stir at $-78\text{ }^\circ\text{C}$ for twenty minutes, the 1,5-dibromopentane (69 g, 41 mL) was added dropwise. The resulting mixture was stirred (3 h) at $-78\text{ }^\circ\text{C}$ before the addition of ammonium chloride (14 g). After further (1 h) stirring at $-78\text{ }^\circ\text{C}$, the cold bath around the reaction flask was removed and the ammonia allowed to slowly evaporate. The next day, water (200 mL) was added to the brown residue in the flask, and the resulting mixture was extracted with diethyl ether ($5 \times 200\text{ mL}$). The combined ethereal extracts were treated with potassium carbonate to remove water before filtration and evaporation to produce a heavy oil. The heavy oil was distilled in vacuum (0.1 mmHg) to provide 1,7-bis-(4-pyridyl) heptane.

Compound 2:

1,7-bis(4-Pyridyl)heptane **1** (0.100 g, 0.463 mmol) was dissolved in ethanol (5 mL) and layered onto a solution of $\text{Cd}(\text{ClO}_4)_2 \cdot x\text{H}_2\text{O}$ (0.121 g, $\sim 0.40\text{ mmol}$) in water (5 mL). The solution was left to stand for two weeks, during which time colourless plates of compound **2** grew at the interface. These crystals were harvested via filtration and air dried (0.148 g, 67%). Found: C 55.3; H 6.2; N 7.4%. $\text{C}_{53}\text{H}_{76}\text{CdCl}_2\text{N}_6\text{O}_{11}$ requires C 55.0; H 6.6; N 7.3%; IR ν_{max} (KBr)/ cm^{-1} 3431s, 3052w, 2929s, 2853s, 1612s, 1558w, 1466w, 1425w, 1224w, 1193s, 1009s, 811w, 625s and 584w.

Compound 3:

1,7-bis(4-Pyridyl)heptane **1** (0.100 g, 0.463 mmol) was dissolved in ethanol (5 mL) and layered onto a solution of $\text{Cd}(\text{NO}_3)_2 \cdot 6\text{H}_2\text{O}$ (0.120 g, 0.389 mmol) in water (5 mL). The

solution was left to stand for two weeks, during which time colourless blocks of compound **3** grew at the layer interface, which were collected and air dried (0.119 g, 54%). IR ν_{\max} (KBr)/ cm^{-1} 2924s, 2856s, 1575s, 1557w, 1502w, 1485s, 1350s, 1226s, 1014s and 810s.

Caution! Cadmium salts are toxic, and perchlorates can be explosive. Work with small quantities, and take all appropriate safety precautions.

2.2. Crystal Structure Determinations

The intensity data for compounds **2** and **3** were collected using a Nonius Kappa CCD diffractometer (Mo $K\alpha$ radiation, $\lambda = 0.71073 \text{ \AA}$, $T = -153 \text{ }^\circ\text{C}$). For compound **2**, a colourless plate of dimensions $0.20 \times 0.15 \times 0.02 \text{ mm}$ was chosen for data collection, and for compound **3**, a colourless block $0.25 \times 0.20 \times 0.15 \text{ mm}$ was used. Empirical (multi-scan) absorption corrections were applied at the data-reduction stage. The crystal of **2** was found to be non-merohedrally twinned, and some overlapped reflections from the two domains were excluded from the refinement. The structures were routinely solved via direct methods using SHELXS-97 [34] (space groups $P2_1$ for compound **2** and $P2_1/n$ for compound **3**), and the atomic models were developed and refined against $|F|^2$ with SHELXL-2019 [35]. The O-bound H atoms in compound **2** were found in difference maps and refined as riding atoms in their as-found relative positions with $U_{\text{iso}}(\text{H}) = 1.2U_{\text{eq}}(\text{O})$. The C-bound H atoms for both structures were geometrically placed and modelled as riding atoms with C–H = $0.95\text{--}0.99 \text{ \AA}$ depending on hybridisation and $U_{\text{iso}}(\text{H}) = 1.2U_{\text{eq}}(\text{C})$. The structures were verified and analysed with PLATON [36], and the molecular graphics were generated with ORTEP-3 [37] and Mercury [38]. Crystal data for compounds **2** and **3** are summarised in Table 1, and selected geometrical data are presented in Tables 2 and 3. Full details can be found in the deposited cif files. Structural data for other MOFs and their ref. codes were accessed using the Cambridge Structural Database [39]. The mode of interpenetration was worked out from the X-Ray single-crystal data [38].

Table 1. Key crystallographic data for compounds **2** and **3**.

	2	3
Empirical formula	$\text{C}_{53}\text{H}_{76}\text{CdCl}_2\text{N}_6\text{O}_{11}$	$\text{C}_{34}\text{H}_{34}\text{CdN}_6\text{O}_6$
M_r	1156.50	745.15
Crystal system	Monoclinic	Monoclinic
Space group	$P2_1$ (No. 4)	$P2_1/n$ (No. 14)
a (\AA)	11.1612 (3)	23.0560 (3)
b (\AA)	16.2897 (5)	7.72740 (10)
c (\AA)	15.3959 (5)	30.3995 (6)
β ($^\circ$)	95.1973 (11)	102.8379 (7)
V (\AA^3)	2787.66 (15)	5280.68 (14)
Z	2	6
ρ_{calc} (g cm^{-3})	1.378	1.406
μ (mm^{-1})	0.550	0.672
Data collected ($2\theta < xx^\circ$)	13,913	19,872
Unique data	13,913	10,201
R_{Int}	–*	0.058
Flack parameter	0.05 (3)	
R (F)	0.078	0.044
wR (F^2)	0.217	0.112
CCDC deposition number	2,405,487	2,405,488

* Data not merged for a non-merohedral twin.

Table 2. Selected geometrical data (Å, °) for compound 2.

Cd1–O1	2.328 (6)		Cd1–N1	2.349 (5)
Cd1–N3	2.350 (6)		Cd1–O2	2.357 (7)
Cd1–N4 ⁱ	2.357 (6)		Cd1–N2 ⁱⁱ	2.359 (6)
C3–C6–C7–C8	61.9 (13)		C6–C7–C8–C9	173.8 (7)
C7–C8–C9–C10	−171.3 (7)		C8–C9–C10–C11	178.9 (7)
C9–C10–C11–C12	74.5 (10)		C10–C11–C12–C15	173.1 (7)
C20–C23–C24–C25	61.7 (10)		C23–C24–C25–C26	−177.8 (7)
C24–C25–C26–C27	178.2 (8)		C25–C26–C27–C28	179.3 (8)
C26–C27–C28–C29	−178.1 (7)		C27–C28–C29–C32	174.8 (7)
C37–C40–C41–C42	174.9 (7)		C40–C41–C42–C43	175.0 (7)
C41–C42–C43–C44	53.8 (11)		C42–C43–C44–C45	163.2 (9)
C43–C44–C45–C46	−69.9 (12)		C44–C45–C46–C49	−171.2 (8)
O1–H1o...O8 ⁱⁱⁱ	0.85	2.03	2.877 (9)	179
O1–H2o...N6 ⁱⁱⁱ	0.84	1.97	2.778 (10)	163
O2–H3o...O6 ^{iv}	0.86	2.09	2.787 (9)	138
O2–H4o...N5 ^v	0.84	2.04	2.760 (10)	144
O11–H11o...O4 ^{vi}	0.84	2.18	3.018 (10)	174
C17–H17...O3 ^v	0.95	2.55	3.253(12)	131
C18–H18...O2	0.95	2.51	3.185 (11)	128
C35–H35...O9 ⁱ	0.95	2.57	3.429 (12)	151
C47–H47...O5 ^{vii}	0.95	2.53	3.422 (13)	156
C51–H51...O9	0.95	2.58	3.376 (11)	141

The four values for the hydrogen bonds refer to the D–H...A and D...A separations (Å) and the D–H...A angle (°), respectively. Symmetry codes: (i) $x, y, z + 1$; (ii) $x, y, z - 1$; (iii) $x + 1, y, z$; (iv) $1 - x, \frac{1}{2} + y, 1 - z$; (v) $1 - x, \frac{1}{2} + y, 2 - z$; (vi) $x - 1, y, z - 1$; (vii) $x - 1, y, z$.

Table 3. Selected geometrical data (Å, °) for compound 3.

Cd1–O1	2.311 (2)		Cd1–N1	2.326 (3)
Cd1–O4	2.350 (2)		Cd1–N5	2.351 (3)
Cd1–N3	2.377 (3)		Cd1–N4 ⁱ	2.385 (3)
Cd2–O7	2.310 (2)		Cd2–O7 ⁱⁱ	2.310 (2)
Cd2–N6 ⁱⁱⁱ	2.331 (3)		Cd2–N6 ^{iv}	2.331 (3)
Cd2–N2	2.370 (3)		Cd2–N2 ⁱⁱ	2.370 (3)
C3–C6–C7–C8	65.2 (4)		C6–C7–C8–C9	170.7 (3)
C7–C8–C9–C10	−55.9 (4)		C8–C9–C10–C11	−53.9 (4)
C9–C10–C11–C12	176.2 (3)		C10–C11–C12–C15	70.0 (4)
C20–C23–C24–C25	−65.4 (4)		C23–C24–C25–C26	−169.1 (3)
C24–C25–C26–C27	66.8 (4)		C25–C26–C27–C28	175.5 (3)
C26–C27–C28–C29	174.1 (3)		C27–C28–C29–C32	176.5 (3)
C37–C40–C41–C42	−173.5 (3)		C40–C41–C42–C43	−172.6 (3)
C41–C42–C43–C44	−64.7 (5)		C42–C43–C44–C45	−170.6 (3)
C43–C44–C45–C46	63.5 (5)		C44–C45–C46–C49	162.3 (3)
C17–H17...N6 ^{iv}	0.95	2.60	3.281 (4)	129
C51–H51...O9 ^v	0.95	2.51	3.297 (4)	140
C2–H2...O4 ^{vi}	0.95	2.50	3.208 (4)	131
C5–H5...O4	0.95	2.57	3.225 (4)	126
C11–H11B...O5 ^{vii}	0.99	2.55	3.434 (4)	148
C12–H12A...O6 ^{vii}	0.99	2.54	3.411 (4)	147
C14–H14...O8 ^{viii}	0.95	2.56	3.203 (4)	125
C47–H47...O7 ⁱⁱⁱ	0.95	2.51	3.191 (4)	129
C47–H47...O8 ⁱⁱⁱ	0.95	2.52	3.438 (4)	163
C18–H18...N4 ⁱ	0.95	2.57	3.232 (4)	127
C24–H24B...O9 ^{ix}	0.99	2.47	3.261 (4)	136
C31–H31...O9 ^x	0.95	2.46	3.351 (5)	157

Table 3. Cont.

C30–H30···O1 ^{xi}	0.95	2.39	3.057 (4)	127
C34–H34···O4 ^{xi}	0.95	2.39	3.069 (4)	128
C46–H46A···O3 ^{xii}	0.99	2.41	3.287 (4)	148

The four values for the hydrogen bonds refer to the $D-H\cdots A$ and $D\cdots A$ separations (Å) and the $D-H\cdots A$ angle ($^\circ$), respectively. Symmetry codes: (i) $\frac{1}{2} - x, y + 3/2, \frac{1}{2} - z$; (ii) $2 - x, 2 - y, -z$; (iii) $2 - x, 1 - y, -z$; (iv) $x, y - 3, z$; (v) $x, y + 3, z$; (vi) $x, y - 1, z$; (vii) $1 - x, -y, -z$; (viii) $2 - x, 1 - y, -z$; (ix) $x - 1, y + 1, z$; (x) $x - 1, y, z$; (xi) $\frac{1}{2} - x, y - 3/2, \frac{1}{2} - z$; (xii) $3/2 - x, y + 3/2, \frac{1}{2} - z$.

3. Results and Discussion

3.1. Structure of Compound 2

The asymmetric unit of compound **2** consists of a Cd^{2+} ion, three $C_{17}H_{22}N_2$ ligands, two perchlorate ions, two water molecules and an ethanol solvent molecule (Figure 2). The cadmium ion is coordinated by four ligand nitrogen atoms (from the N1/N2 and N3/N4 ligands) and two water O atoms to generate a regular *trans*- CdO_2N_4 octahedron (Table 2), with the minimum/maximum *cis* and *trans* bond angles being $81.7(3)/95.5(3)^\circ$ and $171.79(17)/175.7(3)^\circ$, respectively. The bond valence sum (BVS) [40], in valence units, for the metal ion is 1.99, being in very good agreement with the expected value of 2.00.

In the N1/N2 ligand, the dihedral angle between the aromatic rings is $69.5(4)^\circ$. The alkyl chain linking the pyridine rings is characterised by six torsion angles (Table 2). Working from C3 in the N1 ring to C15 in the N2 ring (see Figure 2), the chain has a *gaaaga* conformation, where *g* = *gauche* (modulus of torsion angle lies between 50° and 70°) and *a* = *anti* (modulus of torsion angle $> 170^\circ$). For the N3/N4 ligand, the dihedral angle between the pyridine rings is $80.7(4)^\circ$, and the alkyl-chain conformation is *gaaaaa* (N3 ring \rightarrow N4 ring). For the N5/N6 ligand, which is not bonded to the metal ion, the inter-ring dihedral angle is $33.4(4)^\circ$, and the chain conformation is *aagaga* (N5 ring \rightarrow N6 ring). The deviations of the metal ions from their attached rings with nitrogen atoms N1–N4 are as follows: $0.840(1)$ Å, $-0.069(1)$ Å, $-0.586(1)$ Å and $0.452(1)$ Å. The mean Cl–O bond length in the perchlorate ions in compound **2** is 1.439 Å, which is quite typical [41].

In the extended structure of compound **2**, the N1/N2 and N3/N4 ligands bridge the cadmium nodes into [001] infinite cationic looped chains of formula $[Cd(C_{17}H_{22}N_2)_2(H_2O)]^{2+}_n$ (Figure 3), with a metal–metal separation of $15.3959(10)$ Å, which is much longer than the shortest inter-chain Cd···Cd separation of $9.9070(9)$ Å. There are 32 atoms (two bph ligands and two metal atoms) in each loop of the polymeric chain. These chains stack in the [100] direction to generate (010) *pseudo* layers in the crystal. Sandwiched between the *pseudo* layers are (010) sheets of free ligands (i.e., the N5/N6 molecule), perchlorate anions and ethanol solvent molecules of crystallisation (Figure 4). Hydrogen bonding (Table 2) appears to play an important role in the cohesion of the layers: each water molecule bonded to the cadmium ion partakes in one O–H···O bond to a perchlorate ion and one O–H···N hydrogen bond to a nitrogen atom of the free ligand. Finally, the OH group of the ethanol molecule forms an O–H···O link to a perchlorate ion. There are also several weak C–H···O interactions present.

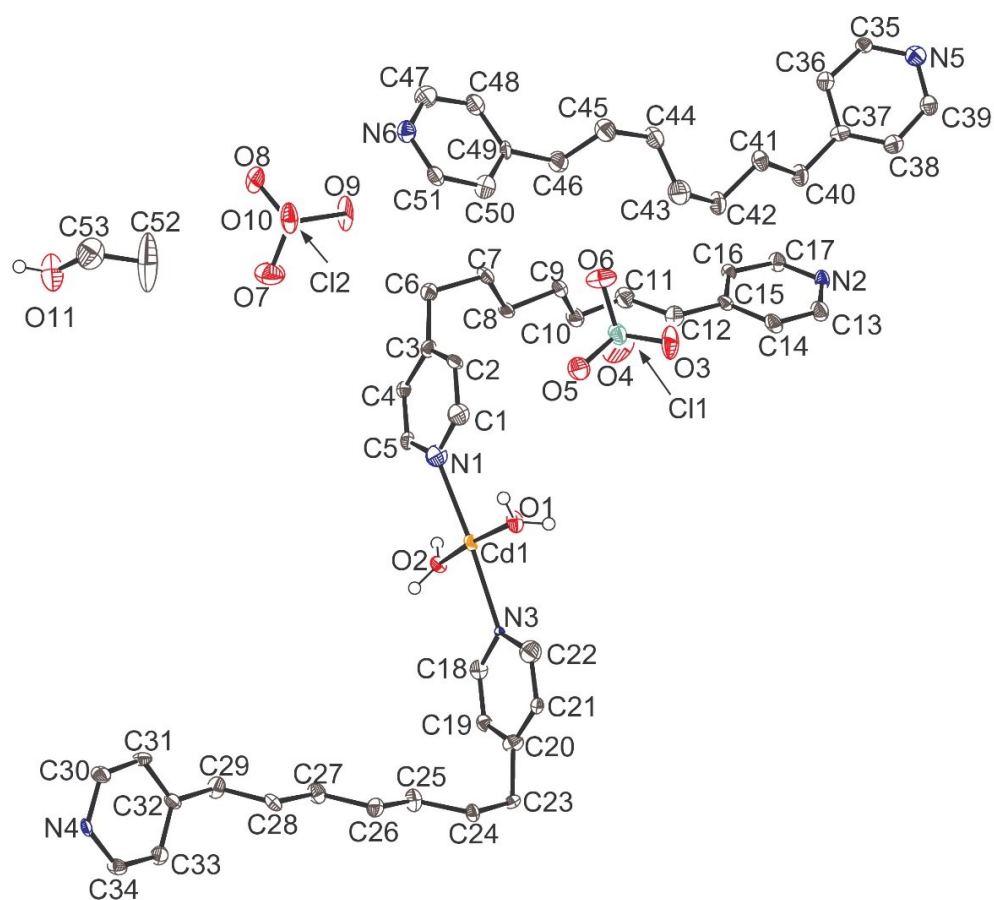


Figure 2. The asymmetric unit of **2**, showing 50% displacement ellipsoids. The C-bound H atoms are omitted for clarity. Red is oxygen, green is chlorine and cadmium is orange.

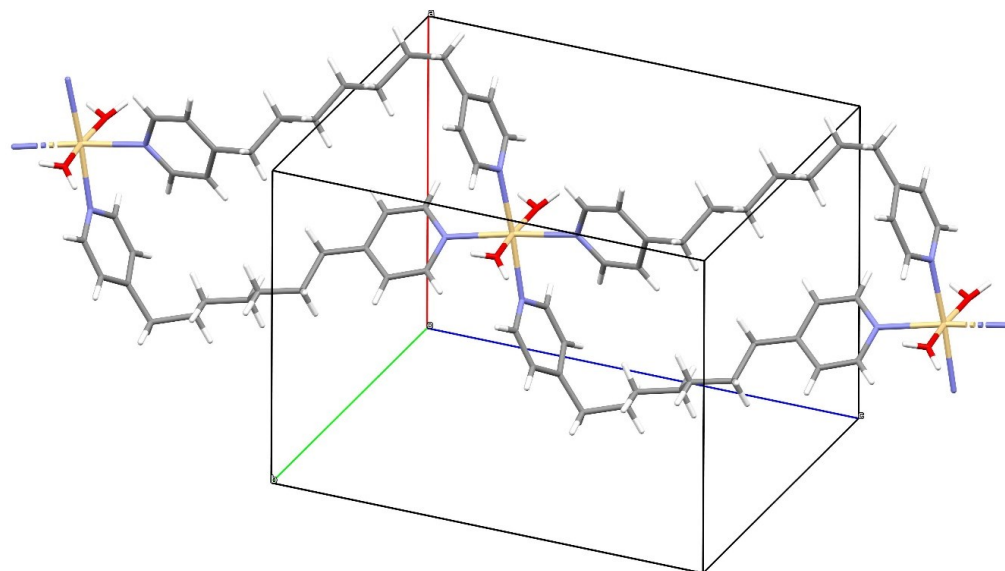


Figure 3. Part of a looped [001] chain in the structure of **2**. In this and subsequent packing figures, the red, green and blue lines indicate the [100] (*a*-axis), [010] (*b*-axis) and [001] (*c*-axis) directions, respectively, with respect to the unit-cell origin, where the coloured lines intersect. The coordinated water is red.

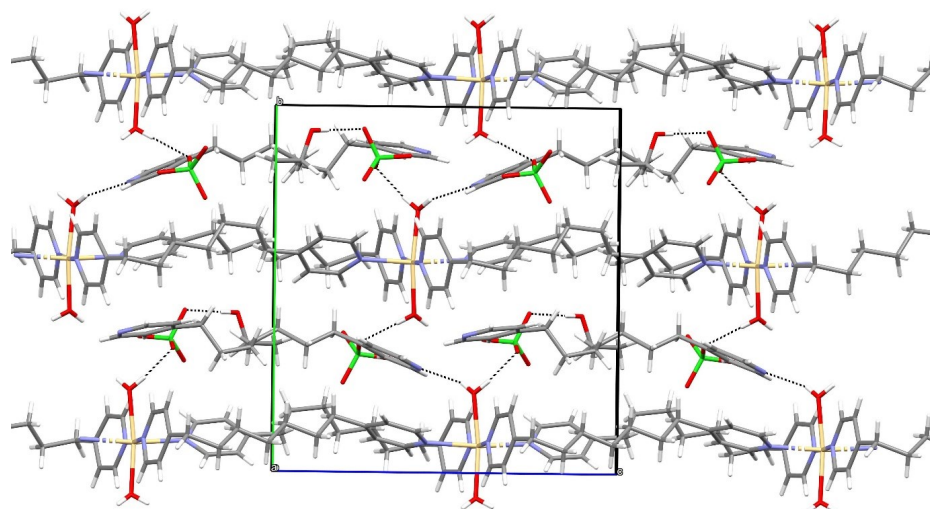


Figure 4. The unit-cell packing for **2** viewed down [100], showing the (010) alternating sheets of $[\text{Cd}(\text{C}_{17}\text{H}_{22}\text{N}_2)_2(\text{H}_2\text{O})_2]^{2+}$ looped chains (at $y \approx 0, \frac{1}{2}$ and 1) and perchlorate ions, free ligands and ethanol solvent molecules (at $y \approx \frac{1}{4}$ and $\frac{3}{4}$). Hydrogen bonds are indicated by black dashed lines. Oxygen is red and and chlorine is green.

3.2. Structure of Compound 3

The asymmetric unit of compound **3** consists of two Cd^{2+} ions (one of which lies on a crystallographic inversion centre), three $\text{C}_{17}\text{H}_{22}\text{N}_2$ ligands and three nitrate anions (Figure 5). This leads to the uncommon situation of $Z = 6$ for a monoclinic crystal based on the simplest empirical formula for **3** of $\text{Cd}(\text{C}_{17}\text{H}_{22}\text{N}_2)_2(\text{NO}_3)_2$. Both the cadmium ions are coordinated by four ligand N atoms and two monodentate nitrate O atoms to generate a fairly regular *trans*- CdO_2N_4 octahedron in each case (Table 3). The bond valence sum for Cd is 2.00 and for Cd2 (site symmetry $\bar{1}$) is 2.06.

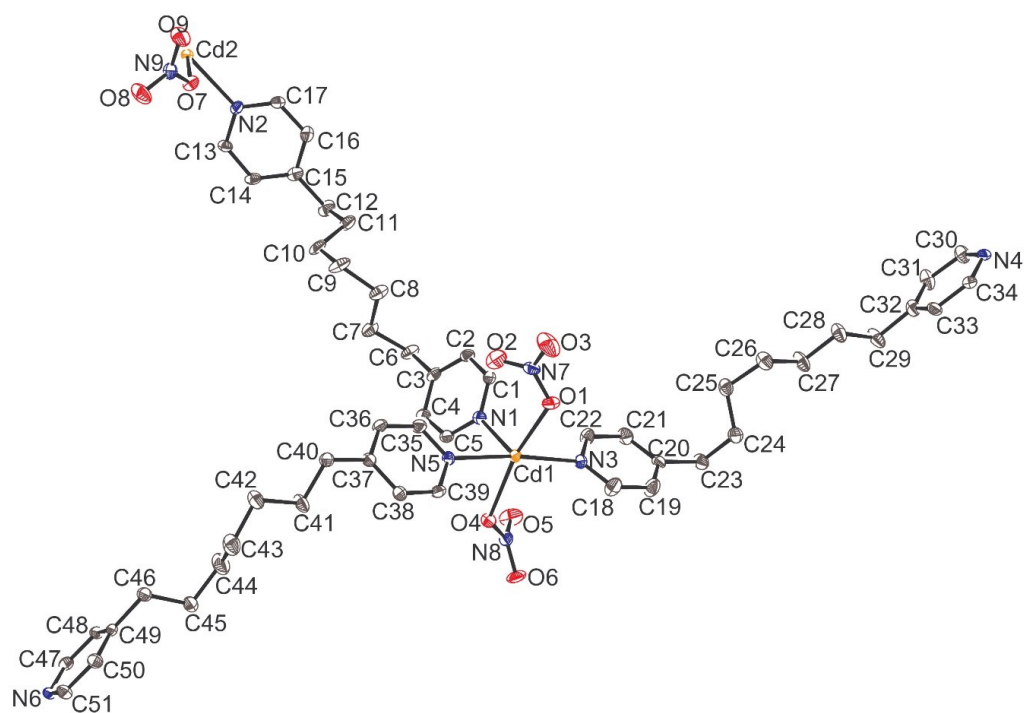


Figure 5. The asymmetric unit of **3**, showing 50% displacement ellipsoids. The H atoms are omitted for clarity. Oxygen is red, nitrogen is blue and cadmium is orange.

In the N1/N2 ligand, the dihedral angle between its aromatic rings is $51.32(12)^\circ$, and the linking $-(CH_2)_7-$ alkyl chain has a *gaggag* conformation (in the sense of progressing from the N1 ring to the N2 ring). The pyridine rings in the N3/N4 ligand subtend a dihedral angle of $60.05(13)^\circ$, and its alkyl-chain conformation is *gagaaa* (N3 ring \rightarrow N4 ring). For the N5/N6 ligand, the inter-ring dihedral angle is $79.45(11)^\circ$, and the chain conformation is *aagaga* (N5 ring \rightarrow N6 ring). The deviations of the metal ions from their attached rings with nitrogen atoms N1–N6, respectively, are as follows: Cd1 = $0.068(5) \text{ \AA}$; Cd2 = $0.378(5) \text{ \AA}$; Cd1 = $0.177(5) \text{ \AA}$; Cd1 = $0.137(5) \text{ \AA}$; Cd1 = $0.074(5) \text{ \AA}$; Cd2 = $0.234(5) \text{ \AA}$. The mean N–O bond length in the nitrate ions for the oxygen atoms (O1, O4 and O7) also bonded to the metal ions of 1.281 \AA is significantly longer than that of the free oxygen atoms (1.233 \AA).

In the extended structure of compound **3**, the three ligand molecules are all bridging to generate a square grid propagating in the (103) plane with a regular 4^4 topology [2,7,8] (Figures 6–8). Each Cd1 atom is linked to two other Cd1 atoms and two Cd2 atoms in a *pseudo "cis"* square planar arrangement; each Cd2 atom is linked to four Cd1 atoms: the Cd \cdots Cd distances within this network are $17.1075(4) \text{ \AA}$, $18.2357(5) \text{ \AA}$ and $18.2592(4) \text{ \AA}$. The shortest out-and-back circuit for both Cd1 and Cd2 encompasses no fewer than 64 atoms (four bph ligands and four metal atoms). The shortest metal \cdots metal separation in the structure of compound **3** of $7.7274(4) \text{ \AA}$ arises due to interpenetration of the 4^4 nets (see below).

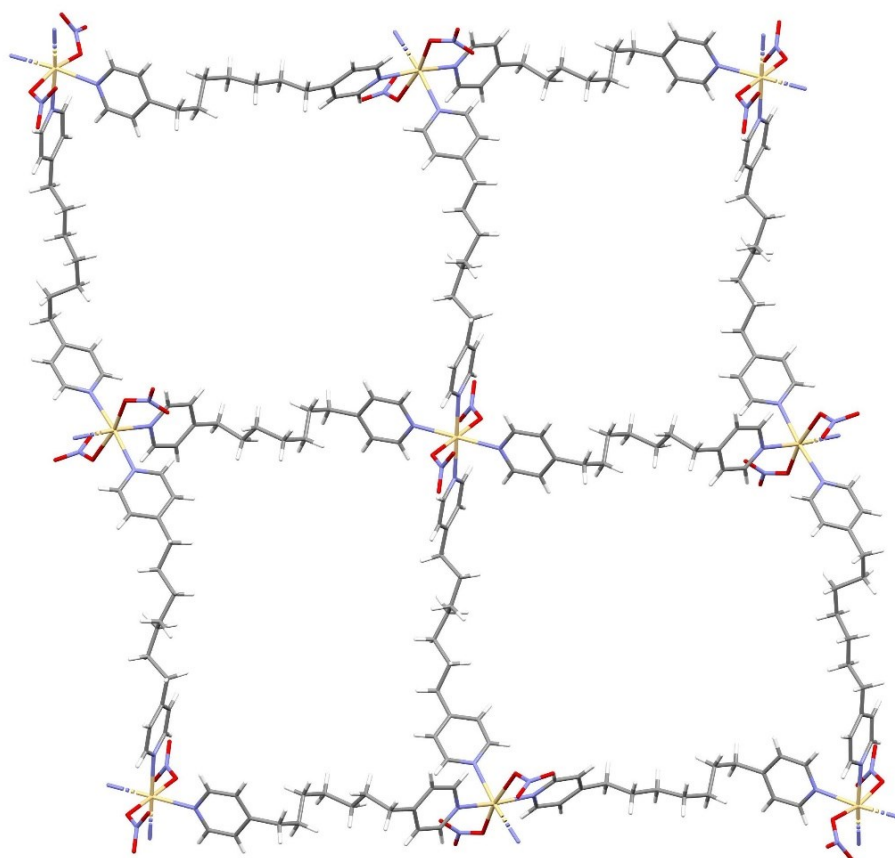


Figure 6. Part of a 4^4 grid in the extended structure of **3**. Oxygen is red, nitrogen is blue and cadmium is yellow.

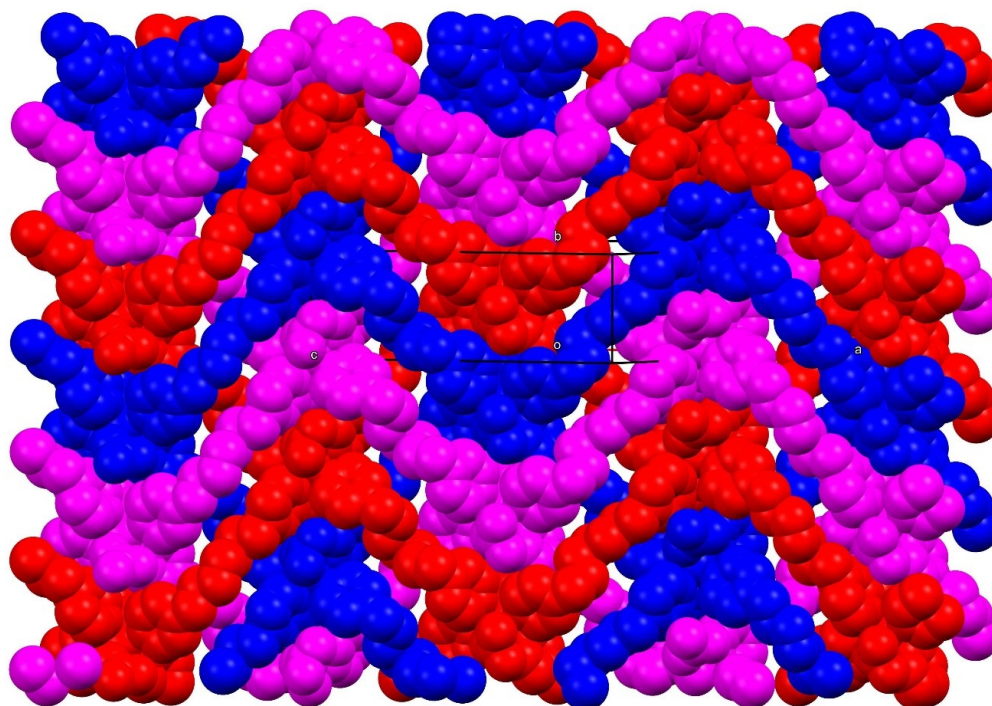


Figure 7. Interpenetrated (103) sheets of 4^4 grids coloured red, purple and blue in the structure of **3**. The three grids alternate in the [010] direction.

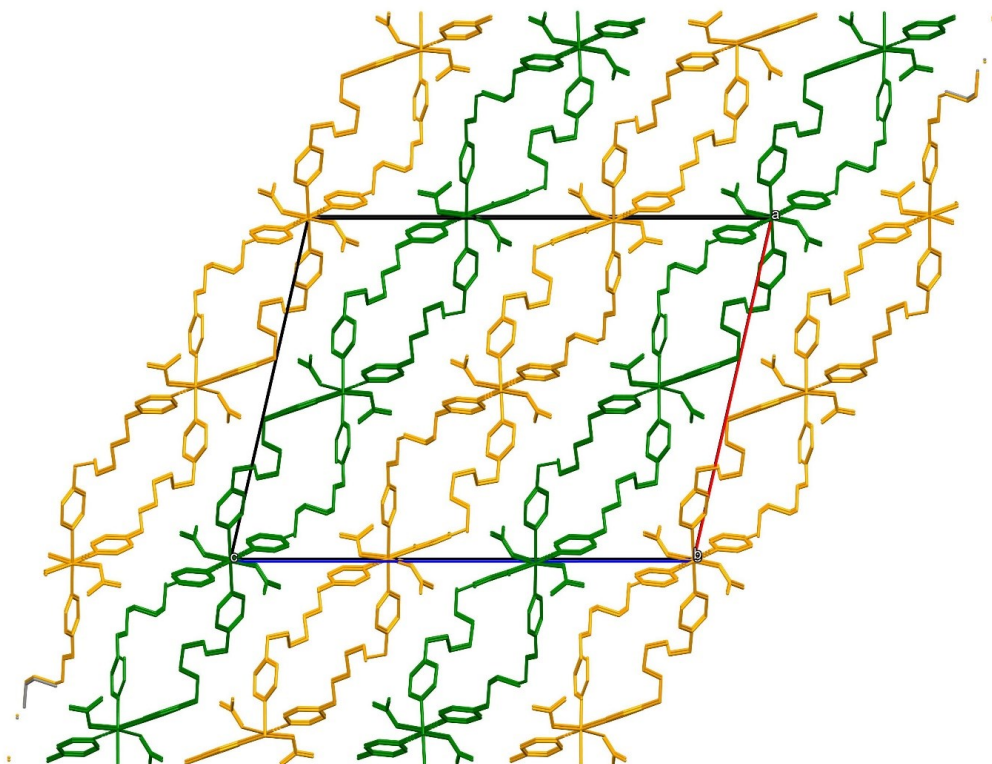


Figure 8. The unit-cell packing in **3** viewed down [010], showing the (103) sheets, which are alternately coloured green and orange for clarity.

The 4^4 nets in compound **2** do not occur in isolation, but a triply interpenetrated layer structure arises, with each infinite 4^4 grid interpenetrated by two others. It may be seen in Figure **6** that the individual grids (coloured red, purple and blue) alternate with respect

to the [010] direction. Finally, the (103) interpenetrated sheets stack together to yield the crystal structure of compound **3** (Figure 7).

4. Conclusions

The syntheses and structures of $[\text{Cd}(\text{C}_{17}\text{H}_{22}\text{N}_2)_2(\text{H}_2\text{O})_2] \cdot 2(\text{ClO}_4) \cdot \text{C}_{17}\text{H}_{22}\text{N}_2 \cdot \text{C}_2\text{H}_5\text{OH}$ **2** and $[\text{Cd}(\text{C}_{17}\text{H}_{22}\text{N}_2)_2(\text{NO}_3)_2]$ **3** have been described. The same metal ion and bridging ligand in combination with different counter-ions has resulted in very different structures. The different geometries of the flexible dph ligands (as quantified by their alkyl chain torsion angles) are notable, with no fewer than five different conformations occurring, as noted above.

$[\text{Cd}(\text{C}_{15}\text{H}_{18}\text{N}_2)_2(\text{H}_2\text{O})_2] \cdot 2(\text{ClO}_4) \cdot \text{C}_{15}\text{H}_{18}\text{N}_2 \cdot \text{C}_2\text{H}_5\text{OH}$ (TOKCON) [7], in which the ligand has two fewer methylene groups, has a very similar formula to that of compound **2**, but its structure is different: TOKCON consists of a squashed two-dimensional 4^4 grid rather than the one-dimensional looped chains seen in **2**, but both contain *trans*- CdO_2N_4 nodes and layers containing free ligands, perchlorate ions and ethanol solvent molecules. The hydrogen-bonding pattern of $\text{O}-\text{H} \cdots \text{O}$ and $\text{O}-\text{H} \cdots \text{N}$ links from the coordinated water molecules is almost the same in both structures.

Compound **3** consists of a novel array of triply interpenetrated 4^4 two-dimensional grids, which is facilitated by the long spacer chain of seven carbon atoms in the bph ligand, which are not disordered. It may be noted that $[\text{Cd}_2(\text{C}_{13}\text{H}_{14}\text{N}_2)_4(\text{NO}_3)_4(\text{H}_2\text{O})]$ (LOPNEJ) [2] where $\text{C}_{13}\text{H}_{14}\text{N}_2$ is the shorter ligand 1,3-bis(4-pyridyl)propane containing three methylene groups, contains doubly interpenetrated 4^4 grids with two different types of *trans*- CdN_4O_2 nodes (one with two nitrate anions and one with one nitrate ion and one water molecule). The fascinating area of interpenetrated MOF structures has recently been reviewed by Gupta and Vittal [41].

Other MOFs containing 1,7-bis(4-pyridyl)heptane characterised by single-crystal diffraction include $[\text{Zn}_2(\text{OH})(\text{C}_{17}\text{H}_{22}\text{N}_2)_2] \cdot 3(\text{ClO}_4) \cdot \frac{1}{2}(\text{H}_2\text{O})$ (WETWOH) [5] (a search for WETWOH in the CSD also matches with a completely different zirconium organometallic compound) and $[\text{Cu}_2(\text{C}_{17}\text{H}_{22}\text{N}_2)_4(\text{NO}_3)_3] \cdot \text{NO}_3 \cdot \text{H}_2\text{O}$ (DITYIP) [6]. WETWOH shows unusual hydroxyl-bridged $\text{Zn}(\text{OH})\text{Zn}$ dimeric units, with one of the distinct ligands bridging the dimers into chains and the other “dangling”, being bonded to the zinc ion from just one of its N atoms: the interpretation of the structure of WETWOH was hindered by severe disorder of the ligands. In DITYIP, the two distinct copper nodes form CuN_4O square-based pyramids and *trans*- CuN_4O_2 Jahn–Teller distorted octahedra. These are linked by the ligands into a triply interpenetrated three-dimensional network based on $(6^5 \cdot 8^2)$ nets [6].

These materials may find applications in gas storage, separation, catalysis and slow-release cadmium materials. The interpenetration networks may become either two or just one network as they crystallise with guest molecules, which stabilise the large framework.

Author Contributions: Conceptualisation, M.J.P., W.T.A.H., M.R.S.J.F. and B.M.D.S.; methodology M.J.P., W.T.A.H., M.R.S.J.F. and B.M.D.S.; software, M.J.P., W.T.A.H., M.R.S.J.F. and B.M.D.S.; validation, M.J.P., W.T.A.H., M.R.S.J.F. and B.M.D.S.; formal analysis M.J.P., W.T.A.H., M.R.S.J.F. and B.M.D.S.; investigation M.J.P., W.T.A.H., M.R.S.J.F. and B.M.D.S.; resources, M.J.P., W.T.A.H., M.R.S.J.F. and B.M.D.S.; data curation, M.J.P., W.T.A.H., M.R.S.J.F. and B.M.D.S.; writing—original draft preparation, M.J.P., W.T.A.H., M.R.S.J.F. and B.M.D.S.; writing—review and editing M.J.P., W.T.A.H., M.R.S.J.F. and B.M.D.S.; visualisation, M.J.P., W.T.A.H., M.R.S.J.F. and B.M.D.S.; supervision, M.J.P.; project administration, M.J.P. All authors have read and agreed to the published version of the manuscript.

Funding: This research received no external funding.

Data Availability Statement: This paper is available at <https://www.abdn.ac.uk/people/m.j.plater> (accessed on 10 December 2024).

Acknowledgments: We thank the EPSRC National Crystallography Service (University of Southampton) for the X-ray data collections.

Conflicts of Interest: The authors declare no conflicts of interest.

References

1. Lee, D.N.; Kim, Y. Two-dimensional structure of poly[[[12-1,4-bis(pyridin-4-yl)butane]bis(14-pentanedioato)dicopper(II)] acetoni-trile disolvate]. *IUCrData* **2017**, *2*, x171448. [[CrossRef](#)]
2. Plater, M.J.; Foreman, M.R.S.J.; Gelbrich, T.; Coles, S.J.; Hursthouse, M.B. Synthesis and characterisation of infinite co-ordination networks from flexible dipyridyl ligands and cadmium salts. *J. Chem. Soc. Dalton Trans.* **2000**, *18*, 3065–3073. [[CrossRef](#)]
3. Li, D.-S.; Zhang, M.-L.; Zhao, J.; Wang, D.-J.; Zhang, P.; Wang, N.; Wang, Y.-Y. A novel 3D Cd^{II}-coordination framework with helical units in a mixed flexible ligand system: Encapsulating right-handed helical water chains. *Inorg. Chem. Commun.* **2009**, *12*, 1027–1030. [[CrossRef](#)]
4. Liu, J.; Zhang, H.-B.; Tan, Y.-X.; Wang, F.; Klang, Y.; Zhang, J. Structural Diversity and Photoluminescent Properties of Zinc Benzotriazole-5-carboxylate Coordination Polymers. *Inorg. Chem.* **2014**, *53*, 1500–1506. [[CrossRef](#)] [[PubMed](#)]
5. Plater, M.J.; Foreman, M.R.S.J.; Gelbrich, T.; Hursthouse, M.B. Synthesis and characterisation of infinite di- and tri-nuclear zinc co-ordination networks with flexible dipyridyl ligands. *J. Chem. Soc. Dalton Trans.* **2000**, *1*, 1995–2000. [[CrossRef](#)]
6. Plater, M.J.; Gelbrich, T.; Hursthouse, M.B.; de Silva, B.M. Interpenetrating three-dimensional coordination networks with a rare 4-connected (6⁵.8) topology and unusual geometrical features. *Cryst. Eng. Comm.* **2008**, *10*, 125–130. [[CrossRef](#)]
7. Harrison, W.T.A.; Plater, M.J.; de Silva, B.M.; Foreman, M.R.S.J. Crystal structure of a layered coordination polymer based on a 4⁴ net containing Cd²⁺ ions and 1,5-bis(pyridin-4-yl)pentane linkers. *Acta Cryst. Sect. E Cryst. Commun.* **2014**, *70*, 80–83. [[CrossRef](#)] [[PubMed](#)]
8. Plater, M.J.; Foreman, M.R.S.J.; Gelbrich, T.; Hursthouse, M.B. Synthesis and characterisation of infinite coordination networks with 1,6-bis(4-pyridyl)hexane and copper nitrate. *Cryst. Eng. Commun.* **2001**, *4*, 319–328. [[CrossRef](#)]
9. Plater, M.J.; de Silva, B.M.; Foreman, M.R.S.J.; Harrison, W.T.A. Crystal structures of two one-dimensional coordination polymers constructed from Mn²⁺ ions, chelating hexafluoro-acetylacetonate anions, and flexible bipyridyl bridging ligands. *J. Struct. Chem.* **2016**, *57*, 1169–1175. [[CrossRef](#)]
10. Plater, M.J.; Foreman, M.R.S.J.; Howie, R.A.; Skakle, J.M.S. Structures of Mn(II) thiocyanate co-ordination polymers from flexible bipyridyl ligands. *Inorg. Chim. Acta* **2001**, *318*, 175–180. [[CrossRef](#)]
11. Plater, M.J.; Foreman, M.R.S.J.; Skakle, J.M.S. Synthesis of co-ordination networks from flexible bis(4-pyridyl) ligands and cadmium salts. *Cryst. Eng.* **2001**, *4*, 293–308. [[CrossRef](#)]
12. Zhang, J.; Kumar Ghosh, M.; Yang, D.-C.; Muddassir, M.; Kumar Ghorai, T.; Jin, J.-C. A new 2,5-bis(pyrid-4-yl)pyridine based Mn(II) metal-organic framework on photochemically antibiotic degradation. *Inorganica Org. Chim. Acta* **2024**, *569*, 122132. [[CrossRef](#)]
13. Mehrlana, G.; Chitsa, V.; Mugazda, T. Recent advances in metal-organic frameworks based on pyridylbenzoate ligands: Properties and applications. *RSC Adv.* **2015**, *5*, 88218–88233. [[CrossRef](#)]
14. Zhao, J.; Wang, Y.-N.; Dong, W.-W.; Wu, Y.-P.; Li, D.-S.; Zhang, Q.-C. A Robust Luminescent Tb(III)-MOF with Lewis Basic Pyridyl Sites for the Highly Sensitive Detection of Metal Ions and Small Molecules. *Inorg. Chem.* **2016**, *55*, 3265–3271. [[CrossRef](#)]
15. Zhang, G.; Zheng, S.; Neary, M.C. An ionic Fe-based metal-organic-framework with 4'-pyridyl-2,2':6',2''-terpyridine for catalytic hydroboration of alkynes. *RSC Adv.* **2023**, *13*, 2225–2232. [[CrossRef](#)]
16. Guo, M.C.; Zhong, W.D.; Wu, T.; Han, W.-D.; Gao, X.-S.; Ren, X.-M. Two Bi-MOFs with pyridylmulticarboxylate ligands showing distinct crystal structures and phosphorescence properties. *J. Sol. State Chem.* **2022**, *309*, 123005. [[CrossRef](#)]
17. Chao, M.Y.; Chen, J.; Wu, X.-Y.; Wang, R.-Y.; Wang, P.-P.; Ding, L.; Young, D.J.; Zhang, W.-H. Unconventional Pyridyl Ligand Inclusion within a Flexible Metal-Organic Framework Bearing an N,N'-Diethylformamide (DEF)-Solvated Cd₅ Cluster Secondary Building Unit. *ChemPlusChem* **2020**, *85*, 503–509. [[CrossRef](#)] [[PubMed](#)]
18. Chen, B.; Wang, L.; Xiao, Y.; Fronczek, F.R.; Xue, M.; Cui, Y.; Qian, G. A Luminescent Metal-Organic Framework with Lewis Basic Pyridyl Sites for the Sensing of Metal Ions. *Angew. Chem. Int. Ed. Eng.* **2009**, *48*, 500–503. [[CrossRef](#)] [[PubMed](#)]
19. Zhao, X.; Su, B.; Zhao, Q.; Lv, W.; Chen, L.; Huang, L.; Li, X.; Liao, S. Construction of pyridine-functionalized metal-organic frameworks for the detection of flazasulfuron. *Acta Cryst.* **2024**, *C80*, 806–814. [[CrossRef](#)] [[PubMed](#)]
20. Ashiry, K.O.; Abbas, R.K. Synthesis and Characterization of a Metal-Organic Framework Bridged by Long Flexible Ligand. *Open J. Poly. Chem.* **2021**, *11*, 1–9. [[CrossRef](#)]
21. Zhang, J.-P.; Zhou, H.-L.; Zhou, D.D.; Liao, P.-Q.; Chen, X.-M. Controlling flexibility of metal-organic frameworks. *Nat. Sci. Rev.* **2018**, *5*, 907–919. [[CrossRef](#)]
22. Zhu, D.; Li, H.; Su, Y.; Jiang, M. Pyridine-containing metal-organic frameworks as precursor for nitrogen-doped porous carbons with high-performance capacitive behavior. *J. Solid State Electrochem.* **2017**, *21*, 2037–2045. [[CrossRef](#)]
23. Xiang, H.; He, Y.; Zhang, Z.; Wu, H.; Zhou, W.; Krishna, R.; Chen, B. Microporous metal-organic framework with potential for carbon dioxide capture at ambient conditions. *Nature Commun.* **2012**, *954*, 1–9. [[CrossRef](#)] [[PubMed](#)]
24. Ganesan, M. Are metal-organic frameworks at a commercial tipping point? *CAS Insights*, 5 December 2024.
25. Arceo-Ruiz, H.; Xochitiotzi-Flores, E.; García-Ortega, H.; Farfán, N.; Santillan, R.; Rincón, S.; Zepeda, A. Synthesis of a New Co Metal-Organic Framework Assembled from 5,10,15,20-Tetrakis((pyridin-4-yl) phenyl)porphyrin “Co-MTPhPyP” and Its Application to the Removal of Heavy Metal Ions. *Molecules* **2023**, *28*, 1816. [[CrossRef](#)] [[PubMed](#)]
26. Zhou, Y. Metal-Organic Framework Based on Pyridine-2,3-Dicarboxylate and a Flexible Bis-imidazole Ligand: Synthesis, Structure, and Photoluminescence. *J. Inorg. Organomet. Polym. Mat.* **2013**, *23*, 458–462. [[CrossRef](#)]

27. Wong-Ng, W.; Culp, J.; Chen, Y.S.; Espinal, L.; Allen, A.J.; Siderius, D.; Brown, C.M.; Queen, W.L.; Zavalij, P.; Matranga, C. Flexible metal organic framework compound, Ni(1,2-bis(4-pyridyl)ethylene)[Ni(CN)₄]_n, for CO₂ sorption applications. Abstracts of Papers. In Proceedings of the 245th ACS National Meeting & Exposition, New Orleans, LA, USA, 7–11 April 2013.
28. Yan, L.; Kuang, G.; Zhang, Q.; Shang, X.; Pei Nian Liu, P.N.; Lin, N. Self-assembly of a binodal metal–organic framework exhibiting a demi-regular lattice. *Faraday Discuss.* **2017**, *204*, 111–121. [[CrossRef](#)] [[PubMed](#)]
29. Abbasi, S.T.A. Metal-organic frameworks of cobalt and nickel centers with carboxylate and pyridine functionality linkers: Thermal and physical properties; precursors for metal oxide nanoparticle preparation. *J. Nanostruct.* **2012**, *2*, 379–388.
30. Siraj, I.T.; Spicer, M.D. Building Metal Organic Frameworks with Pyridine Fuctionalised Imidazolium Salts Spacers. *Int. J. Chem. Eng. Appl.* **2013**, *4*, 199–203. [[CrossRef](#)]
31. Ossila Enabling Science. MOF Ligands for Sale. Available online: <https://www.ossila.com/collections/mof-ligands> (accessed on 10 December 2024).
32. Feng, D.-D.; Zhao, Y.-D.; Wang, X.-Q.; Fang, D.-D.; Tang, J.; Fan, L.-M.; Yang, J. Two novel metal–organic frameworks based on pyridyl-imidazole-carboxyl multifunctional ligand: Selective CO₂ capture and multi-responsive luminescence sensor. *Dalton Trans.* **2019**, *48*, 10892–10900. [[CrossRef](#)]
33. Jampolsky, L.M.; Baum, M.; Kaiser, S.; Sternbach, L.H.; Goldberg, M.W. The Synthesis of 2,2'- and 4,4'-Polymethylenebipyridines. *J. Am. Chem. Soc.* **1952**, *74 Pt 20*, 5222–5224. [[CrossRef](#)]
34. Sheldrick, G.M. *SHELXS97 and SHELXL97*; Programs for Crystal Structure Solution and Refinement; University of Göttingen: Göttingen, Germany, 1997.
35. Sheldrick, G.M. Crystal structure refinement with SHELXL. *Acta Cryst.* **2015**, *C71*, 3–8.
36. Spek, A.L. Structure validation in chemical crystallography. *Acta Cryst.* **2009**, *D65*, 148–155. [[CrossRef](#)] [[PubMed](#)]
37. Farrugia, L.J. *WinGX and ORTEP for Windows*: An update. *J. Appl. Cryst.* **2012**, *45*, 849–854. [[CrossRef](#)]
38. Macrae, C.F.; Sovago, I.; Cottrell, S.J.; Galek, P.T.A.; McCabe, P.; Pidcock, E.; Platings, M.; Shields, G.P.; Stevens, J.S.; Towler, M.; et al. *Mercury 4.0*: From visualization to analysis, design and prediction. *J. Appl. Cryst.* **2020**, *53*, 226–235. [[CrossRef](#)] [[PubMed](#)]
39. Groom, C.R.; Bruno, I.J.; Lightfoot, M.P.; Ward, S.C. The Cambridge Structural Database. *Acta Cryst.* **2016**, *B72*, 171–179. [[CrossRef](#)]
40. Nguyen, T.N. Bond Valence Sum: A Powerful Tool for Determination of Oxidation States of Metal Ions in Coordination Compounds. *ChemRxiv Inorg. Chem.* **2020**, *5*, 1–10.
41. Gupta, M.; Vittal, J.J. Control of interpenetration and structural transformations in the interpenetrated MOFs. *Coord. Chem. Rev.* **2021**, *435*, 213789. [[CrossRef](#)]

Disclaimer/Publisher's Note: The statements, opinions and data contained in all publications are solely those of the individual author(s) and contributor(s) and not of MDPI and/or the editor(s). MDPI and/or the editor(s) disclaim responsibility for any injury to people or property resulting from any ideas, methods, instructions or products referred to in the content.